Effect of arsenic trioxide on cervical cancer and its mechanisms

LIPING ZHANG[1,2*], YANAN ZHOU[3*], JING KONG[3], LI ZHANG[4], MENGQIN YUAN[4], SHU XIAN[4], YANQING WANG[4], YANXIANG CHENG[4] and XIAOFENG YANG[1]

[1]Department of Obstetrics and Gynecology, The First Affiliated Hospital of Xi'an Jiaotong University, Xi'an, Shanxi 710061; [2]Department of Obstetrics and Gynecology, Wuhan Children's Hospital and Wuhan Maternal and Child Healthcare Hospital, Tongji Medical College, Huazhong University of Science and Technology, Wuhan, Hubei 430060; [3]Technology Chemical Engineering of Huaiyin Institute, Huai'an, Jiangsu 223001; [4]Department of Obstetrics and Gynecology, Renmin Hospital of Wuhan University, Wuhan, Hubei 430060, P.R. China

Received November 4, 2019; Accepted July 14, 2020

DOI: 10.3892/etm.2020.9299

Abstract. Cervical cancer is one of the most common types of gynecological tumor, and thus identifying complementary or substitute treatment methods to treat cervical cancer is important. The present study aimed to evaluate the effect of arsenic trioxide (ATO), a traditional Chinese medicine, on cervical cancer cells and its underlying mechanism. MTT, colony formation and Transwell assays were performed to investigate the effects of different concentrations of ATO on cell proliferation and invasion, respectively. Western blotting and reverse transcription-quantitative PCR were applied to measure hypoxia-inducible factor-1α expression (HIF-1α) expression following ATO treatment. Finally, the effects of HIF-1α knockdown on cervical cancer cell proliferation, apoptosis and invasion were evaluated. The results demonstrated that ATO could inhibit cell proliferation and invasion. Moreover, ATO could induce reactive oxygen species production in a time- and dose-dependent manner. ATO could also promote the apoptosis of cervical cancer cells via HIF-1α. Therefore, the present study may provide a theoretical basis for identifying effective molecular targets for the prevention and treatment of cervical cancer.

Correspondence to: Professor Xiaofeng Yang, Department of Obstetrics and Gynecology, The First Affiliated Hospital of Xi'an Jiaotong University, 277 West Yanta Road, Xi'an, Shanxi 710061, P.R. China
E-mail: yxf73@163.com

Professor Yanxiang Cheng, Department of Obstetrics and Gynecology, Renmin Hospital of Wuhan University, 99 Zhang Zhidong Road, Wuhan, Hubei 430060, P.R. China
E-mail: yanxiangCheng@whu.edu.cn

*Contributed equally

Abbreviations: ATO, arsenic trioxide; ROS, reactive oxygen species; HIF-1α, hypoxia-inducible factor-1α

Key words: arsenic trioxide, cervical cancer, reactive oxygen species, hypoxia-inducible factor-1α

Introduction

Cervical cancer is the 4th most common cancer type worldwide and is a prevalent type of malignant tumor in the female reproductive system (1). There are ~500,000 new cases annually worldwide, where the incidence is rising annually with diagnosis being common among younger women (2,3). Surgery plus radiotherapy can significantly improve the treatment effect of early-stage cancer, but for the late stage, the treatment effect of patients with relapse and metastasis remains at the bottleneck stage, and the 1-year survival rate of patients with late-stage cancer is <20% (4,5). Therefore, it is important to identify the molecular pathogenesis of cervical cancer, in order to develop complementary or substitute treatment methods, as well as more effective strategies to prevent cervical cancer, which will be of great theoretical and practical significance to improve the quality of life of patients with this disease worldwide.

Currently, comprehensive treatments, including surgery, lack a breakthrough in the curative effect of advanced and recurrent cervical cancer, and thus researchers have investigated traditional Chinese medicine (6,7). Arsenic is a traditional Chinese medicine that has three inorganic forms: Red arsenic (As_4S_4), yellow arsenic (As_2S_3) and white arsenic [As_2O_3; arsenic trioxide (ATO)], which are produced by oxidation of arsenic at high temperatures (8). In the mid and late 20th century, Chinese scholars first identified that ATO had significant clinical efficacy for the treatment of acute promyelocytic leukemia, and it is now used in clinical practice (9,10). Recently, additional research has examined solid tumors outside the blood system, and observed a good treatment efficacy in response to ATO (11). Previous studies have reported that ATO exerts antitumor effects on various solid tumors, including liver, breast, osteosarcoma and ovarian cancer, and its possible mechanism of action has also been investigated (12-14). However, its efficacy against cervical cancer has yet to be elucidated, where the underlying mechanism of action remain unknown.

Reactive oxygen species (ROS) is a general term for several active substances formed by oxygen, and the metabolism of ROS is closely associated with numerous metabolic regulatory activities, such as glucose metabolism, in the human body (15,16). The vast majority of oxygen accepts four electrons to combine with H^+ to form water, while some oxygen molecules produce ROS in a single-valent reduction form (17). ROS are important signaling molecules that not only regulate the structure and function of blood vessels, but also serve an important role in regulating cell proliferation, migration and differentiation by effecting the cellular proteins, lipids and nucleic acids (18-20).

Previous studies have revealed that hypoxia-inducible factor-1α (HIF-1α) is an important factor in promoting cell proliferation, invasion and metastasis of malignant tumors (21,22). Moreover, ATO can suppress HIF-1α production to serve an antitumor function in lung carcinoma and breast cancer cells (23,24). However, to the best of our knowledge, the relationship of ATO and HIF-1α has been rarely studied in cervical cancer.

The aim of the present study was to identify a novel strategy for the prevention and treatment of cervical cancer. In the present study, the effect of different times and concentrations of ATO treatment on cervical cancer was investigated. SiHa cells were used to examine the IC_{50} of ATO in cervical cancer cells, as well as to assess the effects of ATO on cell proliferation and invasion. Furthermore, ROS and HIF-1α production were detected to elucidate the mechanism of ATO.

Materials and methods

Materials. The SiHa cervical cancer cell line and 293T cells were purchased from Shanghai Bioengineering Co., Ltd. FBS and RPMI-1640 medium were purchased from Gibco (Thermo Fisher Scientific, Inc.), while the BeyoFast™ SYBR-Green quantitative PCR premix Mix kit, Hoechst 33258 Staining kit (cat. no. C0003), RIPA lysis buffer (cat. no. P0013B), bicinchoninic acid (BCA) protein quantitative kit and MTT kit were all purchased from Beyotime Institute of Biotechnology. PVDF 45-μm non-sterile 50/pk membranes were purchased from EMD Millipore. ATO (white) was purchased from Sigma-Aldrich (Merck KGaA) and the Annexin V-FITC/PI double-staining kit (cat. no. 40302ES20) was purchased from Shanghai Yeasen Biotechnology Co., Ltd.

Cell culture and treatment. ATO powder (0.1 g) was dissolved in 10 ml sodium hydroxide (5 mol/l) before the pH of the solution was adjusted to neutral with hydrogen chloride. ATO was wrapped in foil and kept at -4˚C. Before it was used in cell culture, ATO solution was diluted to the appropriate concentrations (0, 5, 10, 15 and 20 μM) with PBS and filtered with a 0.22-μm filter. SiHa cells were cultured in RPMI-1640 medium containing 10% FBS at 5% CO_2, 37˚C and saturated humidity, and the medium was changed once daily. After the cells entered the logarithmic long-term phase of growth, they were digested using 0.25% pancreatin at 37˚C for 3 min. The cells were inoculated into 96-well ($5x10^4$ cells/well), 24-well ($2x10^5$ cells/well) or 6-well ($1x10^6$ cells/well) plates and cultured for 24 h at 37˚C, before being added with different concentrations of ATO (0, 5, 10, 15 and 20 μM) at the indicated time points (0, 6, 12 and 24 h) and incubated at 37˚C.

Proliferation inhibition assay. The cells were inoculated at a density of $1x10^4$ cells/well in 96-well culture plates. Each group had three compound wells and continued to be cultured after adding different concentrations of ATO (0, 5, 10, 15 and 20 μM) for 0, 6, 12 and 24 h. After the culture solution was removed at different time-points, 10 μl MTT (5 mg/ml) was added to the culture. After culturing for 4 h, the culture was terminated. After the culture solution was absorbed, 100 μl DMSO was added to each well at 37˚C for 10 min. The optical density (OD) values of each group were measured at 570 nm using an enzyme labeling instrument (Type no. Sunrise; Tecan Group, Ltd.). The cell survival curves were plotted with the culture time as abscissa and OD as the ordinate.

Detection of ROS content. Intracellular ROS, such as H_2O_2 and •OH, were determined on the basis of fluorescent light detection using an oxidation-sensitive fluorescent probe dye, 2',7'-dichlorodihydrofluorescein diacetate (H_2DCFDA; Invitrogen; Thermo Fisher Scientific, Inc.) (25). The experiment was performed according to the manufacturer's protocols (26). In brief, $1x10^6$ cells were incubated with the indicated concentrations (0, 5, 10, 15 and 20 μM) of ATO for 0, 6, 12 and 24 h at 37˚C. The cells were then washed in PBS and incubated with 20 μM H_2DCFDA at 37˚C for 30 min according to the manufacturer's instruction. Fluorescence was detected at 488 nm excitation wavelength and 525 nm emission wavelength using an enzyme labeling instrument (Type no. Sunrise; Tecan Group, Ltd.).

Colony formation assay. Cells in the logarithmic growth phase were prepared into single-cell suspensions and counted. In total, 1,000 cells were inoculated in each 60-mm culture dish and cultured in a 5% CO_2 incubator for 37˚C. The medium was changed every 3 days and then removed. Cells were washed three times with PBS, fixed with 100% anhydrous methanol for 15 min at room temperature and stained with 0.1% crystal violet solution for 15 min at room temperature. Subsequently, the number of colonies containing >15 cells was counted under a light microscope (magnification, x400; Carl Zeiss AG).

Cell invasion assay. The final mass concentration of Matrigel was adjusted to 1 mg/ml using 4˚C precooled serum-free medium. The upper Transwell chamber with 8-μm pore-size filters (Corning, Inc.) was coated with Matrigel for 3-5 h at 37˚C and set aside after solidification. The cells were collected in each group before $4x10^5$ cells were suspended in 400 μl serum-free medium, and the Transwell culture chamber was inserted into the 24-well culture plate. The cell mixture was added to the upper layer of the chamber, and RPMI-1640 supplemented with 20% FBS was added to the lower layer of the chamber as the chemokine source. The chamber was removed, and the culture liquid was aspirated after 16 h. The upper layer cells were carefully removed, washed twice with PBS and fixed with 100% anhydrous methanol at room temperature for 5 min. Cells were then stained for 5 min with 0.1% crystal violet at room temperature, rinsed gently

Table I. Reverse transcription-quantitative PCR primer information.

Gene	Primer	Primer sequence	Annealing temperature, ˚C
HIF-1α	F	5'-ACAAGTCACCACAGGACAG-3'	56.91
	R	5'-AGGGAGAAAATCAAGTCG-3'	51.46
GAPDH	F	5'-AGGTCGGTGTGAACGGATTTG-3'	62.14
	R	5'-GGGGTCGTTGATGGCAACA-3'	60.75

F, forward; R, reverse; HIF-1α, hypoxia-inducible factor-1α.

with water several times, dried while inverted and mounted with a coverslip and neutral gum. Under a light microscope (magnification x200; Carl Zeiss AG), six visual fields were randomly selected, and the number of cells stained with crystal violet solution (i.e., the number of invasive cells) was counted.

Western blot analysis. The RIPA lysis buffer (including 1 μM PMSF protease inhibitor) was added to SiHa cells at logarithmic growth phase and then placed on ice for 40 min. The supernatant was collected via 13,000 x g centrifugation for 20 min at 4˚C. The total cell protein was obtained, and the protein concentration was determined using the BCA method. After separating the protein (40 μg protein/lane) on a nitrocellulose membrane with 10% SDS-PAGE, membranes were blocked in 5% skimmed milk powder at room temperature for 3 h. Diluted HIF-1α (1:200; cat. no. ab113642; Abcam) or GAPDH monoclonal antibodies (1:200; cat. no. ab8245; Abcam) were then added and the membranes were incubated overnight on a rocker at 4˚C, followed by washing three times with PBS-0.1%Tween-20 (PBST) for 10 min each. The polyclonal goat anti-mouse horseradish peroxidase-conjugated secondary antibody (1:5,000; cat. no. ab6789; Abcam) was added and incubated at 37˚C for 2 h. Membranes were washed three times in PBST for 10 min each time. Odyssey infrared laser scanning imaging (LI-COR Biosciences) and ImageJ 6.0 (National Institutes of Health) were used to analyze the results.

Reverse transcription-quantitative PCR (RT-qPCR) analysis. The total RNA of the SiHa cells from each group was extracted using TRIzol® reagent (Invitrogen; Thermo Fisher Scientific, Inc.), and the RNA purity and concentration were determined using an ultraviolet spectrophotometer (Tecan Group, Ltd.). The RNA to cDNA EcoDry™ Premix (cat. no. 639549; Takara Biotechnology Co., Ltd.) was used to reverse-transcribe RNA to the first chain of cDNA. The temperature protocol is 42˚C 50 min for reverse transcription reaction, 99˚C for 5 min to inactivate the reverse transcriptase and 4˚C to save the reverse transcription product. The cDNA was subsequently used as a template to detect the expression of HIF-1α using the BeyoFast™ SYBR-Green quantitative PCR premix. The thermocycling conditions were as follows: Initial denaturation at 95˚C for 10 min, followed by 40 cycles of 95˚C for 15 sec and 60˚C for 1 min. At the end of the PCR amplification, the melting curve was plotted and the relative expression of HIF-1α was assessed using the $2^{-\Delta\Delta Cq}$ method (27). The primer sequences are presented in Table I.

Construction of HIF-1α knockdown lentivirus plasmid. The recombinant lentivirus plasmid pLKO.1-HIF-1α short hairpin (sh)RNA sequence 1, pLKO.1-HIF-1α shRNA sequence 2 and negative control plasmid pLKO.01-scrambled-shRNA were designed and synthesized by Cyagen Biosciences Inc. 293T cells were cultured in RPMI-1640 medium containing 10% FBS at 5% CO_2, 37˚C. To produce virus, 293T cells ($1.6x10^6$ cells/well) were seeded into 6-well plates prior to transfection. The ratio of pMDL (0.75 μg), VSVG (0.45 μg), and pRSV-Rev plasmids (0.3 μg) were 5:3:2, which were all purchased from Shanghai GeneChem Co., Ltd. The three plasmids aforementioned (total DNA 1.5 μg), recombinant lentivirus plasmid (1.5 μg) and Lipofectamine® 2000 (6 μl; Invitrogen; Thermo Fisher Scientific, Inc.) were then mixed. After being kept at room temperature for 20 min, the mixture was added to the culture medium of 293T cells drop by drop for transfection. The culture medium was replaced with fresh medium after 6 h, which then continued to cultivate for 24 or 48 h. The supernatant was collected and the lentivirus particles were harvested by ultracentrifugation (2 h at 50,000 x g; 4˚C). SiHa cells were infected [multiplicity of infection (MOI)=10]. After 12-16 h, the medium was replaced with fresh medium. The cells were harvested for subsequent experimentation after 48 h. The DNA single-strand template sequences for the two pairs of interference fragments shRNA1 and shRNA2 are as follows: HIF-1α shRNA sequence 1 forward, 5'-CCGGCTGCC CTTACGCAATAAATTGTCCATATTGGTCTGGAACAA GAGATAGCGGTTTTTG-3' and reverse, 3'-AATTCAAAA ACCGCAATTCAAATGTGACACTCTCCGGGTTAATAT GTCATATTGGTCCAGG-5'; and HIF-1α shRNA sequence 2 forward, 5'-TGCAACATTTTATGATTAGACCCACAATCA GTGAGGATCAGATAACGTTATTCGGTTTTTG-3' and reverse, 3'-AATTCAAAAACCAAGTTCTCTACTTCAGTA AAATATGTTCGTGATCAGATTAAAATTCTGG-5'.

Hoechst staining and flow cytometry assay. Cells in the logarithmic growth phase were collected, and a single-cell suspension with a concentration of $2.5x10^4$ cells/ml was generated. Then, a 200 μl suspension was added to each well of a 96-well plate. After the cells adhered, lentivirus (MOI=10) was used to infect SiHa cells, whilst the control group, which was transfected with the negative control lentiviral vector, was set up, with three wells for each group. After incubating for 72 h at 37˚C and 5% CO_2, the culture medium was aspirated and the cells were fixed in 4% precooled paraformaldehyde at 37˚C for 30 min and stained at 37˚C with Hoechst 33258 staining solution for 5 min (28). The cells were then observed and imaged using

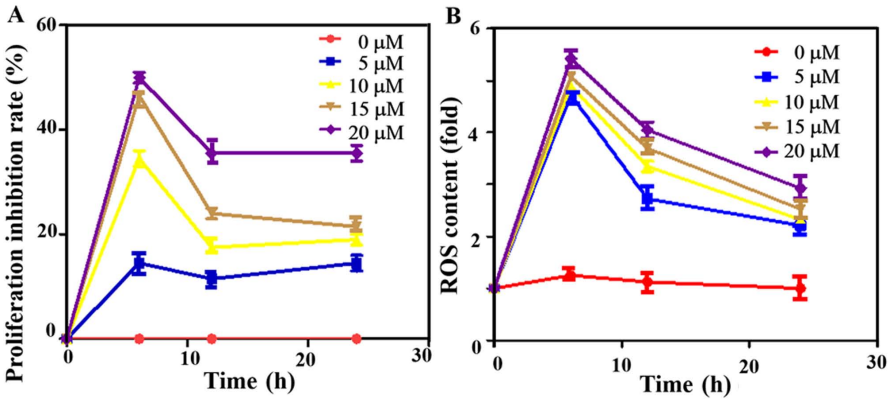

Figure 1. Cell proliferation inhibition rate and ROS content in cells. (A) Proliferation inhibition rate and (B) ROS content in SiHa cells at different time and with various arsenic trioxide concentrations (0, 5, 10, 15 and 20 μM). ROS, reactive oxygen species.

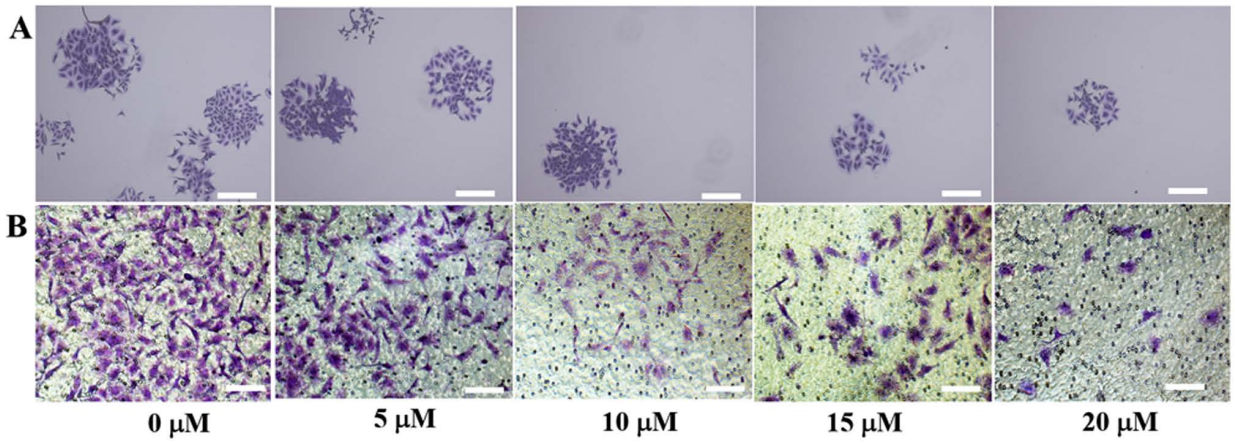

Figure 2. Colony formation assay and cell invasion. Influence of arsenic trioxide on SiHa cell (A) colony-formation capability, scale bar, 200 μm and (B) cell invasive ability, scale bar, 400 μm.

fluorescence microscopy (magnification, x200). For the flow cytometry detection, SiHa cells infected with lentivirus were harvested, washed with PBS and stained with a Annexin V-FITC and PI double-staining kit for 15 min for 37˚C (29). Subsequently, these cells were analyzed via flow cytometry (BD FACSCalibur™; BD Biosciences) within 1 h. The results were evaluated by CellQuest Pro software (version 5.0; BD Biosciences). The apoptotic rate was calculated by the percentage of early and late apoptotic cells.

Statistical analysis. All experiments were repeated three times. Data are presented as the mean ± SD. Unpaired t-test was used to compare two groups, and one-way ANOVA followed by Bonferroni post hoc test was used to compare multiple groups. $P<0.05$ was considered to indicate a statistically significant difference. All data were analyzed using the SPSS 20 (IBM Corp.) software.

Results

Cell viability inhibition rate and ROS content in cells. The 50% inhibitory concentrations (IC_{50}) is the dose of ATO against proliferation of cervical cancer cells within the prescribed time (30). The cell viability inhibition rate was measured using the MTT method after the cells were treated at different ATO concentrations (0, 5, 10, 15 and 20 μM), which demonstrated the inhibition rate to be dependent on the concentration, with the highest rat observed in the 20 μM group. Besides, it was found that with the prolongation of time, the inhibition rate of the ATO first increased, then decreased (Fig. 1A). Subsequently, the inhibition rate remained at a relatively stable level. At 6 h, the inhibition rate was highest in all groups. Thus, ATO had a time- and dose-dependent effect on cell viability.

After the cells were treated with different ATO concentrations for 0, 6, 12 and 24 h, the intracellular ROS content was detected. The ROS content first increased and then decreased in a time- and dose-dependent manner, and it was the highest at 6 h, which suggested that ATO inhibited the proliferation of cervical cancer cells by mainly relying on ROS production (Fig. 1B).

Colony formation assay and cell invasion. SiHa cells were treated with different concentrations ATO for 6 h, the colony formation and Transwell assays were performed to detect cell proliferation and invasion (Fig. 2A and B). When there was no drug treatment, the colony-forming ability of the cells was increased, whilst higher drug concentrations led

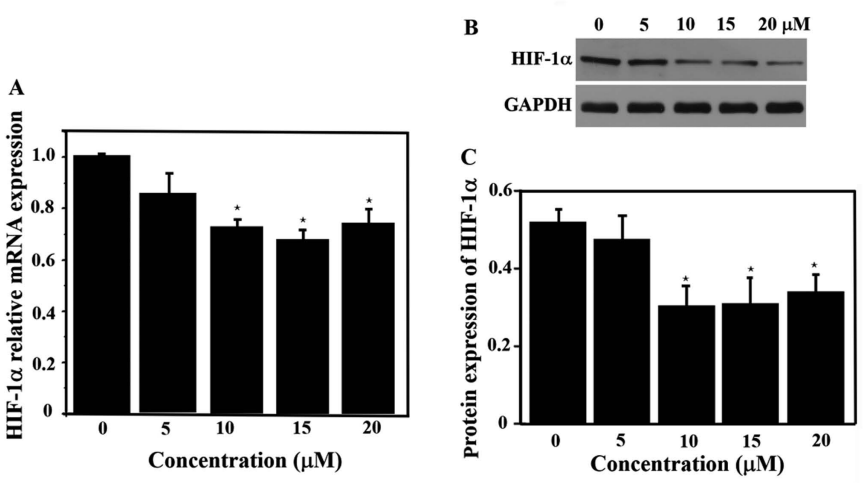

Figure 3. HIF-1α expression with ATO treatment. SiHa cells were cultured for 6 h after treatment with different concentrations of ATO. (A) mRNA expression of HIF-1α. (B) Protein expression of HIF-1α and (C) semi-quantitative and statistical analysis of western blotting. *P<0.05 vs. 0 μM. ATO, arsenic trioxide; HIF-1α, hypoxia-inducible factor-1α.

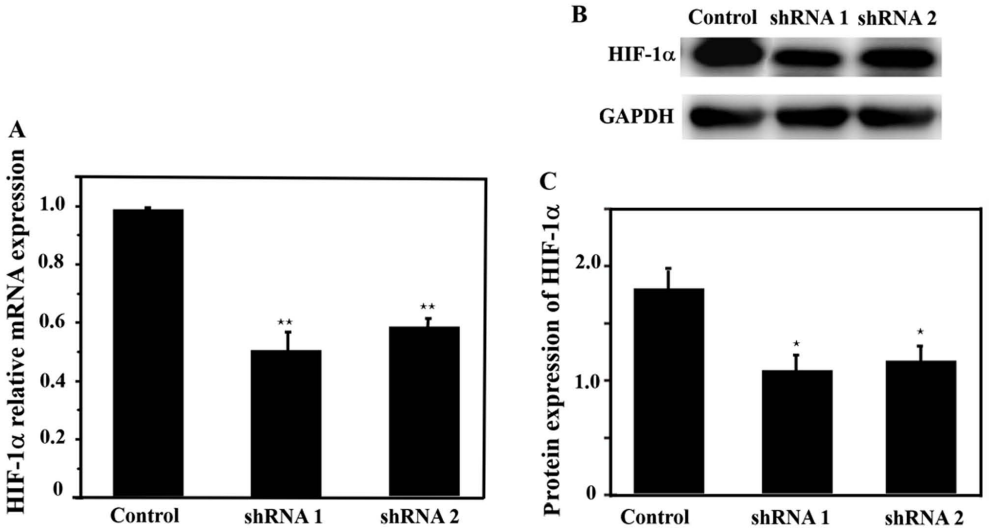

Figure 4. Efficiency of HIF-1α knockdown. After extracting RNA from SiHa cells infected with lentivirus for 72 h, (A) the mRNA expression of HIF-1α and (B) protein expression of HIF-1α were measured. (C) Semi-quantitative and statistical analysis of western blotting. *P<0.05, **P<0.01 vs. control. HIF-1α, hypoxia-inducible factor-1α; shRNA, short hairpin RNA.

to markedly fewer numbers of cell colonies and lowered the invasive capabilities of cells. Therefore, the results suggested that ATO inhibited SiHa cell proliferation and invasion in a dose-dependent manner.

HIF-1α expression with ATO treatment. The relative expression of HIF-1α mRNA was measured with different concentrations ATO. The expression of HIF-1α mRNA was significantly lower in the drug-treated groups (10, 15 and 20 μM) compared with the control group (P<0.05), but there was no significant difference in the expression of HIF-1α mRNA among these three experimental groups (Fig. 3A). Thus, ATO significantly inhibited the expression of HIF-1α mRNA at 6 h. The expression of HIF-1α protein was also significantly lower in the 10, 15 and 20 μM groups (Fig. 3B and C) compared with that in the control group, which was in line with the RT-qPCR results for HIF-1α mRNA expression.

Colony formation and cell migration after knockdown of HIF-1α. HIF-1α mRNA and protein expression levels were detected after infection with lentivirus. The expression levels of HIF-1α mRNA and protein were significantly lower in the HIF-1α shRNA 1 and shRNA 2 groups compared with the control group (Fig. 4). Moreover, HIF-1α shRNA 1 demonstrated a higher inhibitory effect compared with shRNA 2. Therefore, HIF-1α shRNA 1 was selected for subsequent experiments.

The results of the colony formation and cell migration experiments are presented in Fig. 5. Compared with the control group, the number of colonies formed in the HIF-1α knockdown group was markedly lower, indicating that the knockdown of the HIF-1α gene inhibited cell proliferation (Fig. 5A). Furthermore, the cell invasion rate was significantly decreased, suggesting that knocking down HIF-1α reduced the cell invasive ability (Fig. 5B and C).

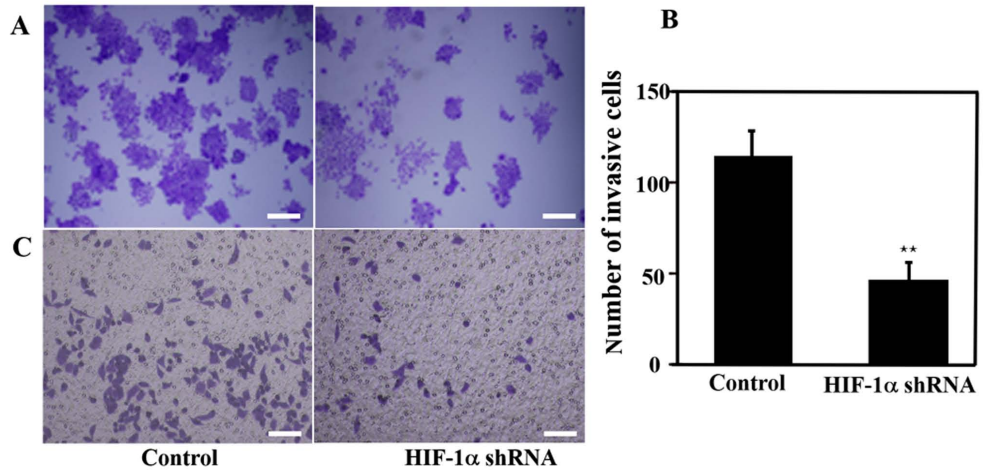

Figure 5. Colony formation and cell migration after knockdown of HIF-1α. (A) Influence of HIF-1α knockdown on SiHa cell colony-formation capability. (B) Quantitative and statistical analysis of SiHa cell invasion. (C) Representative images of invasive SiHa cells. **P<0.01 vs. control. HIF-1α, hypoxia-inducible factor-1α; shRNA, short hairpin RNA.

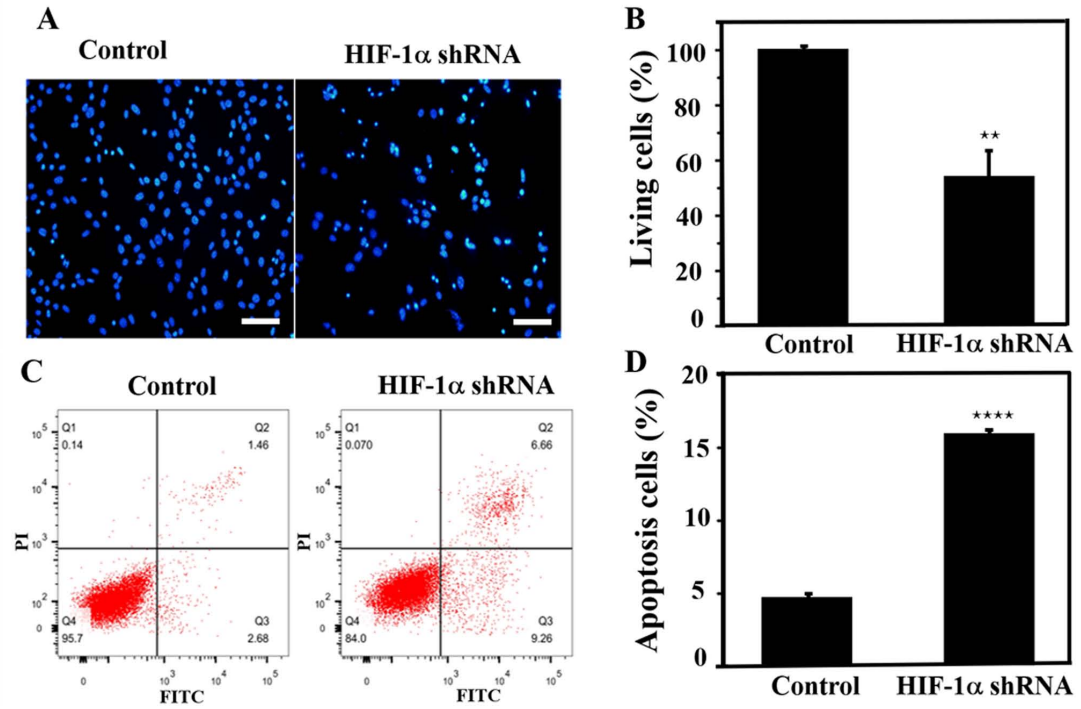

Figure 6. Apoptosis assay after HIF-1α knockdown. Effect of HIF-1α knockdown on apoptosis of SiHa cells using (A) Hoechst staining, (B) quantification of results, as well as (C) flow cytometry and (D) quantification of results. Scale bar, 400 μm. **P<0.01, ****P<0.0001 vs. control. HIF-1α, hypoxia-inducible factor-1α; shRNA, short hairpin RNA.

Apoptosis assay after HIF-1α knockdown. Lentivirus-infected SiHa cells were stained with Hoechst dye after 72 h. SiHa cells exhibited typical morphological changes indicating apoptosis, such as nuclear condensation and nucleosome and nuclear fragmentation, following knockdown of the HIF-1α gene (Fig. 6A). In addition, the apoptotic rate of cells after knockdown was ~50%, demonstrating that HIF-1α knockdown promoted cell apoptosis (Fig. 6B). Flow cytometric analysis was performed to further evaluate apoptosis, and it was identified that after knocking down the HIF-1α gene, the early and late apoptotic rate of SiHa cells was increased by ~3-fold compared with that in the control group (Fig. 6C and D), which was consistent with the aforementioned Hoechst staining results.

Discussion

Cervical cancer is one of the most common gynecological malignancies, which tends to be diagnosed in younger women, and ~570,000 cases of cervical cancer and 311,000 deaths from the disease occurred in 2018 (31). The estimated age-standardized incidence of cervical cancer was 13·1 per 100,000 women globally (31). There is currently no established standard for

effective treatment, and there is yet no commonly accepted highly effective drug. At present, the main treatment principles for cervical cancer are surgery, followed by radiotherapy and chemotherapy (32). Chemotherapy is of great significance in the treatment of cervical cancer, but the main application of chemotherapeutic drugs is not targeted therapy and there are a number of side effects (33). Chemotherapeutic resistance is a major challenge of recurrence and metastasis of cervical cancer (33). Therefore, identifying novel, high-efficiency and low-toxicity chemotherapy drugs will be the primary direction of future research (28,33).

ATO is extracted from the traditional Chinese medicine white arsenic, which is easy to obtain, cost-effective and convenient (34). Recent studies have reported that ATO not only serves an important role in the treatment of hematological malignancies, but also has a beneficial antitumor efficacy in solid tumors (11-13). However, its specific mechanism of action requires further investigation.

ATO-induced apoptosis is a complex process involving multiple targets, and is one of its main antitumor effects (35). Previous studies have revealed that the antitumor effect of ATO is closely associated with ROS (36,37). Moreover, the baseline levels of ROS can stimulate the mitosis, DNA synthesis and the proliferation of tumor cells (38). However, a high level of ROS can induce tumor cell apoptosis and cause tumor cell necrosis (39). It has been reported that an important early cell activity in ATO treatment of target cells is the change in the ROS level, and ATO can increase the level of ROS in cells by acting on multiple pathways, including the ATM-ATR-associated Chk pathway and caspase-3-dependent apoptosis (37,40). However, the exact mechanism of action of ATO in cervical cancer is yet to be fully elucidated (41).

In the present study, different concentrations of ATO were applied to SiHa cells to detect the inhibitory effect of ATO on cellular processes. The results demonstrated that the inhibition rate of 20 μM ATO was ~50% when the cells were treated for 6 h, and the inhibitory effect of ATO on cells was time- and dose-dependent. The level of ROS produced by ATO was also time- and dose-dependent, which indicated that ATO inhibited cervical cancer cellular functions via inducing ROS production in a time- and dose-dependent manner.

HIF-1α is an important factor in determining the prognosis of malignant tumors. For instance, excessive activation of this factor can promote the proliferation, infiltration and metastasis of tumor cells, as well as induce tumor cell resistance to chemotherapy and radiotherapy (42). However, to the best of our knowledge, the relationship of ATO and HIF-1α has been rarely studied in cervical cancer. In the present study, it was identified that ATO could inhibit the expression of HIF-1α, and that the knockdown of HIF-1α can effectively suppressed SiHa cell proliferation and invasion, and promote cell apoptosis.

In conclusion, with regards to the mechanism of action of ATO against cervical cancer, the present results suggested that ATO may inhibit cell proliferation and migration via inducing ROS and inhibiting HIF-1α production. The present study may provide a further theoretical basis for identifying effective molecular targets for the prevention and treatment of cervical cancer. However, the mechanism via which ATO induces ROS and suppresses HIF-1α, and its downregulation of cervical cancer are yet to be elucidated. In addition, additional animal experiments need to further verify the safety of ATO.

Acknowledgements

Not applicable.

Funding

The present study was supported by the Independent Scientific Research Project of Wuhan University (grant no. 413000117) and the Chinese Medical Association Clinical Research Fund-Reproductive Medicine Young Physicians Research and Development Project (grant no. 17020310700).

Availability of data and materials

The datasets used and/or analyzed during the current study are available from the corresponding author on reasonable request.

Authors' contributions

LZ, YZ, YC and XY conceived and designed the research. LZ, YZ, JK, YW, SX, LZ and MY conducted the experiments. All authors analyzed and interpreted the data. All authors read and approved the final version of the manuscript.

Ethics approval and consent to participate

Not applicable.

Patient consent for publication

Not applicable.

Competing interests

The authors declare that they have no competing interests.

References

1. Chen Y, Liu C, Xie B, Chen S, Zhuang Y and Zhang S: miR96 exerts an oncogenic role in the progression of cervical cancer by targeting CAV1. Mol Med Rep 22: 543-550, 2020.
2. Global Burden of Disease Cancer Collaboration; Fitzmaurice C, Dicker D, Pain A, Hamavid H, Moradi-Lakeh M, MacIntyre MF, Allen C, Hansen G, Woodbrook R, *et al*: The global burden of cancer 2013. JAMA Oncol 4: 505-527, 2015.
3. Wei KR, Chen WQ, Zhang SW, Zheng RS, Wang YN and Liang ZH: Epidemiology of uterine corpus cancer in some cancer registering areas of China from 2003-2007. Zhonghua Fu Chan Ke Za Zhi 6: 445-451, 2012 (In Chinese).
4. Sousa DMDN, Chagas ACMA, Vasconcelos CTM, Stein AT and Oriá MOB: Development of a clinical protocol for detection of cervical cancer precursor lesions. Rev Lat Am Enfermagem 26: e2999, 2018.
5. McClung NM, Gargano JW, Park IU, Whitney E, Abdullah N, Ehlers S, Bennett NM, Scahill M, Niccolai LM, Brackney M, *et al*: Estimated number of cases of high-grade cervical lesions diagnosed among women-United States, 2008 and 2016. MMWR Morb Mortal Wkly Rep 68: 337-343, 2019.
6. Su M, Gong XJ and Zhou X: Research progress in mechanism of traditional Chinese medicine active ingredients against cervical cancer. Zhongguo Zhong Yao Za Zhi 44: 675-684, 2019 (In Chinese).

7. Yang J, Li J, Sun M and Chen K: Studies of traditional Chinese medicine monomer on HeLa cell of cervical cancer. Pak J Pharm Sci 27 (4 Suppl): S1063-S1068, 2014.
8. Zhu J, Chen Z, Lallemand-Breitenbach V and de Thé H: How acute promyelocytic leukaemia revived arsenic. Nat Rev Cancer 2: 705-713, 2002.
9. Shen ZX, Chen GQ, Ni JH, Li XS, Xiong SM, Qiu QY, Zhu J, Tang W, Sun GL, Yang KQ, *et al*: Use of arsenic trioxide (As2O3) in the treatment of acute promyelocytic leukemia (APL): II. Clinical efficacy and pharmacokinetics in relapsed patients. Blood 89: 3354-3360, 1997.
10. Wang ZY and Chen Z: Acute promyelocytic leukemia: From highly fatal to highly curable. Blood 111: 2505-2515, 2008.
11. Kozono S, Lin YM, Seo HS, Pinch B, Lian X, Qiu C, Herbert MK, Chen CH, Tan L, Gao ZJ, *et al*: Arsenic targets Pin1 and cooperates with retinoic acid to inhibit cancer-driving pathways and tumor-initiating cells. Nat Commun 9: 3069, 2018.
12. Sadaf N, Kumar N, Ali M, Ali V, Bimal S and Haque R: Arsenic trioxide induces apoptosis and inhibits the growth of human liver cancer cells. Life Sci 205: 9-17, 2018.
13. Wu B, Tan M, Cai W, Wang B, He P and Zhang X: Arsenic trioxide induces autophagic cell death in osteosarcoma cells via the ROS-TFEB signaling pathway. Biochem Biophys Res Commun 1: 167-175, 2018.
14. Wang H, Gao P and Zheng J: Arsenic trioxide inhibits cell proliferation and human papillomavirus oncogene expression in cervical cancer cells. Biochem Biophys Res Commun 441: 556-561, 2014.
15. Jambunathan N: Determination and detection of reactive oxygen species (ROS), lipid peroxidation, and electrolyte leakage in plants. Methods Mol Biol 639: 292-298, 2010.
16. Wang G, Li Y, Yang Z, Xu W, Yang Y and Tan X: ROS mediated EGFR/MEK/ERK/HIF-1α loop regulates glucose metabolism in pancreatic cancer. Biochem Biophys Res Commun 500: 873-878, 2018.
17. Zhao RZ, Jiang S, Zhang L and Yu ZB: Mitochondrial electron transport chain, ROS generation and uncoupling (Review). Int J Mol Med 44: 3-15, 2019.
18. Lu L, Dong J, Wang L, Xia Q, Zhang D, Kim H, Yin T, Fan S and Shen Q: Activation of STAT3 and Bcl-2 and reduction of reactive oxygen species (ROS) promote radioresistance in breast cancer and overcome of radioresistance with niclosamide. Oncogene 37: 5292-5304, 2018.
19. Diwanji N and Bergmann A: An unexpected friend-ROS in apoptosis-induced compensatory proliferation: Implications for regeneration and cancer. Semin Cell Dev Biol 80: 74-82, 2018.
20. Sun X, Jia H, Xu Q, Zhao C and Xu C: Lycopene alleviates H2O2-induced oxidative stress, inflammation and apoptosis in bovine mammary epithelial cells via the NFE2L2 signaling pathway. Food Funct 10: 6276-6285, 2019.
21. Zhang Y, Yan J, Wang L, Dai H, Li N, Hu W and Cai H: HIF-1α promotes breast cancer cell MCF-7 proliferation and invasion through regulating miR-210. Cancer Biother Radiopharm 32: 297-301, 2017.
22. Lai HH, Li JN, Wang MY, Huang HY, Croce CM, Sun HL, Lyu YJ, Kang JW, Chiu CF, Hung MC, *et al*: HIF-1α promotes autophagic proteolysis of Dicer and enhances tumor metastasis. J Clin Invest 128: 625-643, 2018.
23. Sun RC, Board PG and Blackburn AC: Targeting metabolism with arsenic trioxide and dichloroacetate in breast cancer cells. Mol Cancer 10: 142, 2011.
24. Yang MH, Zang YS, Huang H, Chen K, Li B, Sun GY and Zhao XW: Arsenic trioxide exerts anti-lung cancer activity by inhibiting angiogenesis. Curr Cancer Drug Targets 14: 557-566, 2014.
25. Han YH, Kim SH, Kim SZ and Park WH: Caspase inhibitor decreases apoptosis in pyrogallol-treated lung cancer Calu-6 cells via the prevention of GSH depletion. Int J Oncol 5: 1099-1105, 2008.
26. Hsin IL, Ou CC, Wu TC, Jan MS, Wu MF, Chiu LY, Lue KH and Ko JL: GMI, an immunomodulatory protein from Ganoderma microsporum, induces autophagy in non-small cell lung cancer cells. Autophagy 7: 873-882, 2011.
27. Livak KJ and Schmittgen TD: Analysis of relative gene expression data using real-time quantitative PCR and the 2(-Delta Delta C(T)) method. Methods 25: 402-408, 2001.
28. Dueñas-González A and Campbell S: Global strategies for the treatment of early-stage and advanced cervical cancer. Curr Opin Obstet Gynecol 28: 11-17, 2016.
29. Liu H, Pei G, Song M, Dai S and Wang Y: Influence of hsa-miR-6727-5p on the proliferation, apoptosis, invasion and migration of Caski, Hela and SiHa cervical cancer cells. J BUON 22: 973-978, 2017.
30. Sakai C, Arai M, Tanaka S, Onda K, Sugiyama K and Hirano T: Effects of arsenic compounds on growth, cell-cycle distribution and apoptosis of tretinoin-resistant human promyelocytic leukemia cells. Anticancer Res 34: 6489-6494, 2014.
31. Arbyn M, Weiderpass E, Bruni L, de Sanjosé S, Saraiya M, Ferlay J and Bray F: Estimates of incidence and mortality of cervical cancer in 2018: A worldwide analysis. Lancet Glob Health 8: e191-e203, 2020.
32. Menderes G, Black J, Schwab CL and Santin AD: Immunotherapy and targeted therapy for cervical cancer: An update. Expert Rev Anticancer Ther 16: 83-98, 2016.
33. Geretto M, Pulliero A, Rosano C, Zhabayeva D, Bersimbaev R and Izzotti A: Resistance to cancer chemotherapeutic drugs is determined by pivotal microRNA regulators. Am J Cancer Res 7: 1350-1371, 2017.
34. Kuo YJ, Liu YJ, Way TD, Chiang SY, Lin JG and Chung JG: Synergistic inhibition of leukemia WEHI-3 cell growth by arsenic trioxide and Hedyotis diffusa Willd extract *in vitro* and *in vivo*. Exp Ther Med 13: 3388-3396, 2017.
35. Lunghi P, Giuliani N, Mazzera L, Lombardi G, Ricca M, Corradi A, Cantoni AM, Salvatore L, Riccioni R, Costanzo A, *et al*: Targeting MEK/MAPK signal transduction module potentiates ATO-induced apoptosis in multiple myeloma cells through multiple signaling pathways. Blood 112: 2450-2462, 2008.
36. Sarkar S, Mukherjee S, Chattopadhyay A and Bhattacharya S: Low dose of arsenic trioxide triggers oxidative stress in zebrafish brain: Expression of antioxidant genes. Ecotoxicol Environ Saf 107: 1-8, 2014.
37. Qu H, Tong D, Zhang Y, Kang K, Zhang Y, Chen L and Ren L: The synergistic antitumor activity of arsenic trioxide and vitamin K2 in HL-60 cells involves increased ROS generation and regulation of the ROS-dependent MAPK signaling pathway. Pharmazie 68: 839-845, 2013.
38. Hassani S, Ghaffari SH, Zaker F, Mirzaee R, Mardani H, Bashash D, Zekri A, Yousefi M, Zaghal A, Alimoghaddam K and Ghavamzadeh A: Azidothymidine hinders arsenic trioxide-induced apoptosis in acute promyelocytic leukemia cells by induction of p21 and attenuation of G2/M arrest. Ann Hematol 92: 1207-1220, 2013.
39. Pollak M: Targeting oxidative phosphorylation: Why, when, and how. Cancer Cell 23: 263-264, 2013.
40. Kim JH, Kim JH, Yu YS, Kim DH, Kim CJ and Kim KW: Antitumor activity of arsenic trioxide on retinoblastoma: Cell differentiation and apoptosis depending on arsenic trioxide concentration. Invest Ophthalmol Vis Sci 50: 1819-1823, 2009.
41. Chayapong J, Madhyastha H, Madhyastha R, Nurrahmah QI, Nakajima Y, Choijookhuu N, Hishikawa Y and Maruyama M: Arsenic trioxide induces ROS activity and DNA damage, leading to G0/G1 extension in skin fibroblasts through the ATM-ATR-associated Chk pathway. Environ Sci Pollut Res Int 24: 5316-5325, 2017.
42. Su W, Huang L, Ao Q, Zhang Q, Tian X, Fang Y and Lu Y: Noscapine sensitizes chemoresistant ovarian cancer cells to cisplatin through inhibition of HIF-1α. Cancer Lett 350: 94-99, 2011.